Behavior of the chemical potential in calcite and magnesite crystals: A damped harmonic oscillation

On the behaviour of the chemical potential in calcite and magnesite crystals: a damped harmonic oscillation

BRUNO Marco,* RUBBO Marco, MASSARO Francesco Roberto

Dipartimento di Scienze della Terra, Università degli Studi di Torino, Via Valperga Caluso 35, I-10125, Italy

***Corresponding author**
E-mail: marco.bruno@unito.it
Phone: (39) 0116705124
Fax: (39) 0116705128

Abstract

The behaviour of the chemical potential of the species $CaCO_3$ and $MgCO_3$ in proximity of the (10.4) crystal face of calcite and magnesite, is determined at quantum-mechanical level by adopting a recent calculation strategy conceived in our research laboratory. A very peculiar trend of this quantity from the (10.4) surface to the center of the calcite and magnesite crystals was observed. The highest value of the chemical potential is related to the surface layer, while the lowest one is in correspondence to the underlying layer. Interestingly, the chemical potential converges to the bulk value via a damped oscillatory behaviour (DOB). We observed that such DOB is strongly related to the structural modification of the slab caused by the presence of the surface, which produces a damped oscillating behaviour of the interplanar distances, $d_{10.4}$, very similar to the one described for the chemical potential. The implications of this finding are discussed.

1. Introduction

The *chemical potential* of a chemical species (also known as *partial free energy*) is the most important thermodynamic quantity, to understand and describe equilibrium and kinetics processes involving solids and fluids. Therefore, the ability of calculating such a quantity is also of paramount importance to gain more insights on crystal growth processes.

As concerns crystalline phases, a huge amount of experimental work has been done and continues to be done to determine their thermodynamic properties (i.e., enthalpy, entropy, heat capacity) (e.g., see Holland and Powell[1] and references therein). In the last two decades improvements in computing capability and the development of accurate computational codes have

also allowed the investigation of the thermodynamics of minerals with *ab initio* quantum-mechanical methodologies (e.g., Hickel et al.,[2] Wentzcovitch et al.,[3] Gillan et al.[4]). However, these experimental and computational approaches only investigated the thermodynamic properties of the bulk of the crystal and, as a consequence, they exclusively allowed the determination of the chemical potential of an infinite (ideal) crystal. This implies that the chemical potential, at given pressure (*P*) and temperature (*T*), is supposed constant inside the phase. But in the case of a finite (real) crystal limited by {hkl} forms, the chemical potential in proximity of a surface must be higher than that at the center of the crystal: then, a chemical potential gradient is always present inside a real crystal. The constancy of the chemical potential is surely a valid approximation for equilibrium thermodynamic calculations among bulk phases. Instead, for kinetics processes occurring at the interface (e.g., crystal growth and dissolution), considering the bulk value of the chemical potential in place of that at the crystal surface could lead to erroneous interpretations for two reasons: the surfaces break the symmetry of the crystal field and the chemical potential depends on the kind of surface.

Two recent papers[5,6] have addressed the problem of the calculus of the thermodynamic properties of a real crystal, by developing a computational strategy for determining the free energy density (J/m^3) of a crystal, which is related to the chemical potential by a simple scale factor. To date, a first contribution to the determination of the chemical potential of a real crystal was recently given by Bruno and Prencipe,[5] who conceived a new calculation methodology for determining the vibrational contribution of each layer forming the slab, i.e., how the vibrational free energy density at the temperature *T* varies within the slab (the slab is a slice of crystal delimited by two parallel (*hkl*) faces). Their model uses the frequencies of the vibrational modes of the slab and a weight function taking into account how the vibrational amplitude of the atoms involved in the vibrational mode is modified by the presence of the surface. Successively, Bruno[6] developed a calculation method to determine the *static energy contribution at 0K* of each layer forming the slab (i.e., the potential energy density profile); the static and vibrational energies allow one to describe the Helmholtz free energy density profile. In these papers, this new computational method was applied to the study of some crystal faces of calcite ($CaCO_3$). In detail, the free energy density profiles across the (10.4), (10.0) and (01.2) slabs of calcite were determined and discussed, and very interesting features of these density profiles were observed, in particular: (i) the highest and lowest values of the free energy density are always in correspondence of the first (i.e., the layer in contact with the vacuum) and second/third layer of the slab, respectively; (ii) furthermore, the free energy density of the second/third layer is always lower than that of the bulk of the crystal (i.e., the center of the slab). While the first feature was clearly expected, the second one is quite surprising, mainly

because it implies that the chemical potential of the $CaCO_3$ molecules forming the second/third layer of the slab is lower than the chemical potential of the $CaCO_3$ molecules of an infinite crystal.
It is important to stress here that these results[5,6] were obtained by performing the calculations at empirical level by means of the calcite force field developed by Rohl et al.[7] Therefore, to validate them it is needed to use a more accurate *quantum-mechanical* approach. Then, in this paper we determined at *ab initio* level how the chemical potential of the $CaCO_3$ formula unit (f.u.) varies inside a (10.4) slab of calcite and compared these results to the ones obtained at empirical level. To further understand the behaviour of the chemical potential inside a crystal, we also carried out the calculations, at *ab initio* level, on the (10.4) slab of magnesite ($MgCO_3$). The two cases will be described and compared in the following paragraphs. Finally, the chemical potentials of the two phases will be put in relation with the structural variations of the slabs.

2. Results and discussions

2.1. The chemical potential of a finite crystal

The Helmholtz free energy (F) of a finite crystal (i.e., a crystal with constant volume delimited by crystallographic {hkl} forms) is usually described by the relation:

$$F = \sum_i \mu_i n_i + \sum_j \gamma_j A_j \quad (1)$$

where μ_i (J/mol) and n_i are the chemical potential and the number of moles of the i-th species (i.e., atom or molecule; in the present paper the chemical species considered are the $CaCO_3$ and $MgCO_3$ f.u.) forming the crystal, respectively; γ_j is the free surface energy (J/m^2) of the j-th crystal face having area A_j. In eq (1) the edge energy is neglected, as it is noteworthy lower than the term of surface energy. μ_i is the chemical potential of the *bulk crystal*, that is the chemical potential of the i-th species in an infinite crystal. An alternative way to describe the free energy of a crystal is the following:

$$F = \int f(x,y,z)dV \quad (2)$$

where $f(x,y,z)$ is the free energy density of the crystal (J/m^3), which is a function of the position inside the crystal. Obviously, such a variation is a consequence of the crystal surfaces that affect the structural and thermodynamic properties of the inner crystal. It is interesting to observe that the

surface energy of the *j*-th crystal face can be calculated by integrating the function *f(x,y,z)* along a linear path having a direction described by a vector perpendicular to the *j*-th face ($\vec{l}_j$):

$$\gamma_j = \int_a^b f(\vec{l}_j) dl_j \quad (3)$$

where *a* and *b* are two points lying on the path integration and they are located at the center and at the surface of the crystal, respectively. The relation (3) holds for a macroscopic crystal for which the edges effects are negligible and the crystal faces can be simulated with the slab strategy.

The eq. (2) implies the knowledge of how the chemical potential μ_i varies inside the crystal, from the surface to the bulk. The next paragraph will detail the procedure for determining this quantity.

2.2. How to calculate the chemical potential

To investigate the thermodynamic behaviour of a surface, a 2D periodic slab model[8] and the *ab initio* CRYSTAL code[9-11] were adopted. The calculations were performed by using the B3LYP Hamiltonian,[12-14] which provided accurate results for the surface properties of calcite.[15] We used the all Gaussian-type basis sets recently developed by Peintinger et al.[16] for O, C and Ca. It consists of a TZVP contraction that has been systematically derived for solid state systems starting from def2-TZVP[17,18] basis sets devised for molecular cases. Instead, magnesium was described by (8*s*)-(511*sp*)-(1*d*) contractions.[19] Further computational details (e.g., thresholds controlling the accuracy of the calculations) are reported as Supporting Information.

The slabs of a given thickness were made by cutting their respective bulk structures parallel to the *hkl* planes of interest (i.e., 10.4 for calcite and magnesite). Then, the slab geometry (atomic coordinates and 2D cell parameters) was optimized by considering all the atoms free to move. The slab was generated preserving the center of inversion to ensure the vanishing of the dipole moment perpendicular to the slab. The CRYSTAL output files, listing the optimized fractional coordinates and optimized 2D cell parameters of the slabs, are freely available at http://mabruno.weebly.com/download. The calculations were done by considering slabs with a thickness sufficient to obtain an accurate description of the surfaces. The slab thickness is considered appropriate when the bulk-like properties are reproduced at the centre of the slab. In the present work, a slab of eleven layers (*j* = 0,…, 10) was used both for calcite and magnesite.

By using the calculation method developed by Bruno and Prencipe[5] and Bruno,[6,a] it is not possible to extract from the slab optimized with CRYSTAL the chemical potential of the *i*-th species (J/mol of f.u.) in the *j*-th layer of a slab a constant volume and at the temperature *T*, $\mu_i^j(T)$, but the Helmholtz free energy of each f.u. forming the slab, $F_i^j(T)$. Nevertheless, as we will demonstrate in the next paragraph, the difference between $F_i^j(T)$ and $\mu_i^j(T)$ is very small and, as a consequence, we are authorized to assume that $F_i^j(T) \equiv \mu_i^j(T)$. In particular, (i) the static contribution at 0K, $\mu_i^{j,0}$, and the thermal contribution (i.e., vibrational energy and entropy) at the temperature of interest *T*, $\mu_i^{j,T}$, are determined in an independent way, allowing to evaluate their relative weight; (ii) the chemical potential of each f.u. forming the slab (in the present case, 22 $CaCO_3$ f.u. and 22 $MgCO_3$ f.u.) can be evaluated, obtaining in this way information on how the surface affects the chemical potential of the f.u. in the layers forming the slab. A detailed description of the calculation method is not reported in this contribution, since it has been widely explained in our previous papers.[5,6]

At present we only carried out the calculations on crystals having a very simple chemical composition and where only a chemical species is present ($CaCO_3$ or $MgCO_3$). But this typology of work can be extended on whatever crystal, the applicability to more complex systems being exclusively limited by the computational effort needed to optimize the slab structure and determine the vibrational frequencies. Furthermore, this calculation method[5,6] can be applied to the study of the interfaces in epitaxial systems and twinned crystals, as well as to evaluate the effect of the surface defects (e.g., steps, vacancies, dislocations) on the chemical potential of the different chemical species forming a crystal.

2.3. How to estimate the difference between free energy per f.u. and chemical potential

We estimate this quantity by performing an explicit calculation of $\left(\partial F / \partial n\right)$ and $\left(F / n\right)$ for a crystal supposed to be a cube made by $n = m^3$ f.u. (i.e., a cube with *m* identical molecules per edge). If the area occupied by a molecule is *a* and there are m^2 molecules on the area of the face of the cube, the whole area of the crystal is $A = 6am^2$. Then, the Helmholtz free energy of this crystal can be written as:

$$F = \mu n + \gamma A \quad (4)$$

[a] In the paper by Bruno,[6] the eq. (2) is wrong. The correct one is the following: $E_j^0 = E_j + \frac{1}{2}\sum_{i=1, i\neq j}^{n}\left[E_{j,i} - \left(E_j - E_i\right)\right]$.

where μ is the chemical potential of the molecule in an infinite crystal and γ is the free surface energy of the cube face. By dividing eq. (4) by $n = m^3$ and using the relation $A = 6am^2$, one obtains the free energy per molecule:

$$F_n = \left(\frac{F}{n}\right) = \mu + \frac{6a\gamma}{m} \quad (5)$$

Instead, by deriving eq. (4) with respect to *n*, one obtains the chemical potential of the molecule:

$$\mu_n = \left(\frac{\partial F}{\partial n}\right) = \mu + \gamma\left(\frac{dA}{dn}\right) \quad (6)$$

where γ was considered a constant. Then, since we can use the relation $\left(dA/dn\right) = \left(dA/dm\right)\left(dm/n\right) = 4a/m$, eq. (6) becomes:

$$\mu_n = \mu + \frac{4a\gamma}{m} \quad (7)$$

Now, we are able to calculate:

$$\Delta = \mu_n - F_n = \frac{2a\gamma}{m} \quad (8)$$

which furnishes the error we commit in considering $\mu_n \equiv F_n$ in this work. Indeed, by multiplying eq. (8) by the Avogadro's number and inserting in it the (10.4) free surface energy of calcite at 298K (see later for its determination), γ = 0.459 J/m^2, the area occupied by a $CaCO_3$ f.u. in the (10.4) surface of the slab, $a = 2.1\times10^{-19}$ m^2, and the number of $CaCO_3$ f.u. along the z direction of the slab, m = 11, we obtain $\Delta \cong 10^4$ J/mol. Δ is five order of magnitude lower than the values we calculated for $F^{j}_{CaCO3}(298)$ (Fig. 1), that is Δ modifies the $F^{j}_{CaCO3}(298)$ values by ~0.0005%, a variation negligible when compared to the uncertainties related to the functional, basis sets and computational parameters adopted in our calculations.

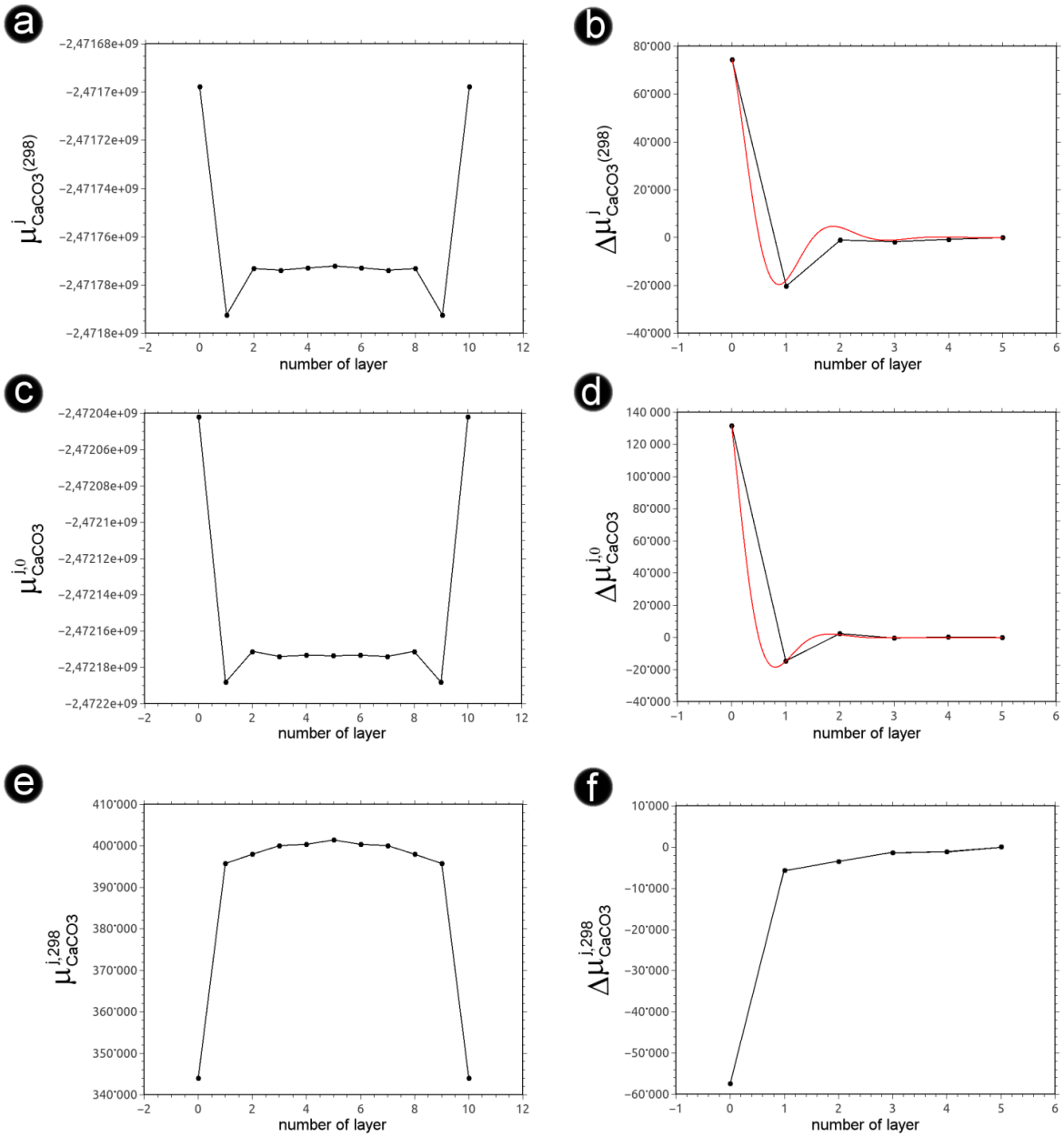

Figure 1. The chemical potential of $CaCO_3$ at 298K (a), $\mu^{j}_{CaCO3}(298)$, its static contribution at 0K (c), $\mu^{j,0}_{CaCO3}$, and its thermal contribution (i.e., vibrational energy and entropy) at 298K (e), $\mu^{j,298}_{CaCO3}$, are reported for each layer j = 0, …, 10 forming the (10.4) slab. The quantities $\Delta\mu^{j}_{CaCO3}(298) = \mu^{j}_{CaCO3}(298) - \mu^{5}_{CaCO3}(298)$ (b), $\Delta\mu^{j,0}_{CaCO3} = \mu^{j,0}_{CaCO3} - \mu^{5,0}_{CaCO3}$ (d) and $\Delta\mu^{j,298}_{CaCO3} = \mu^{j,298}_{CaCO3} - \mu^{5,298}_{CaCO3}$ (f) are also reported. All of the quantities are expressed in J/mol. $\Delta\mu^{j}_{CaCO3}(298)$ and $\Delta\mu^{j,0}_{CaCO3}$ are fitted (red line) with a damped oscillating function, see the main text.

2.4. The chemical potential in the (10.4) slab of calcite

In Fig. 1 $\mu^{j}_{CaCO3}(298)$, $\mu^{j,0}_{CaCO3}$ and $\mu^{j,298}_{CaCO3}$ are reported; in Table S1 (Supporting Information) the numerical values are listed. The highest value of $\mu^{j}_{CaCO3}(298)$ is associated to the surface ($\mu^{0}_{CaCO3}(298) = -2.47169770\times10^{9}$ J/mol), while the lowest one is in correspondence to layer 1 ($\mu^{1}_{CaCO3}(298) = -2.47179244\times10^{9}$ J/mol). Then, $\mu^{j}_{CaCO3}(298)$ rapidly converges to a constant value, which is nothing else that the chemical potential of the crystal bulk ($\mu^{5}_{CaCO3}(298) \equiv \mu^{bulk}_{CaCO3}(298) = -2.47177215\times10^{9}$ J/mol). $\mu^{0}_{CaCO3}(298)$ and $\mu^{1}_{CaCO3}(298)$ are, respectively, ~0.003% and ~0.001% higher and lower than $\mu^{bulk}_{CaCO3}(298)$. It is worth to stress that the convergence to the bulk value proceeds via a damped oscillatory behaviour (DOB), which is more evident when observing Fig. 1b (and Tables S1 and S3, Supporting Information), where $\Delta\mu^{j}_{CaCO3}(298) = \mu^{j}_{CaCO3}(298) - \mu^{bulk}_{CaCO3}(298)$ is plotted (full black circle) and the points are fitted by the relation (red line):

$$\Delta\mu^{j}_{CaCO3}(298) = \Delta\mu^{0}_{CaCO3}(298)\exp(-Aj)\cos(\pi j) \quad (9)$$

where A = 1.4302098 is the damping coefficient, which is determined with the fitting procedure implemented in the software QtiPlot (http://www.qtiplot.com).

The eq. (9) was also used to fit the static quantities $\Delta\mu^{j,0}_{CaCO3} = \mu^{j,0}_{CaCO3} - \mu^{bulk,0}_{CaCO3}$ (Fig. 1d); in this case the damping coefficient is A = 2.1868587, which is higher than that determined for $\Delta\mu^{j}_{CaCO3}$. We want to underline that eq. (9) has not the pretension to describe in an exact way (i.e., *quantitatively*) the behaviour of the chemical potential, but it is only used to show that the trend of μ^{j}_{CaCO3}, from surface to the center of the slab (Table S1), can be represented *qualitatively* with a function suitable to describe the behaviour of a damped harmonic oscillator.

A very different behaviour is instead observed for the thermal part of the chemical potential, $\mu^{j,298}_{CaCO3}$ (Figs. 1e and 1f): there is a monotonic increase of this contribution from the surface to the center of the slab. In particular, $\mu^{0,298}_{CaCO3}$ = 3.44077256×10^{5} J/mol is lower by 13.1% and 14.3% with respect to $\mu^{1,298}_{CaCO3}$ and $\mu^{5,298}_{CaCO3} \equiv \mu^{bulk,298}_{CaCO3}$, respectively. The thermal contribution results to be about four order of magnitude lower with respect to the static one.

The DOB is strongly associated to the structural modification of the slab caused by the presence of the surface, which produces strong variations of the interplanar distances. In Fig. 3a such a distances ($d^{j}_{10.4}$) are plotted for the whole slab, whereas in Fig. 3b the quantity

$\Delta d^{j}_{10.4} = d^{j}_{10.4} - d^{bulk}_{10.4}$ is reported. Interestingly, a damping behaviour very similar to the one described for the chemical potential arises, which can be represented by means of the relation:

$$\Delta d^{j}_{10.4} = \Delta d^{0}_{10.4} \exp(-Aj)\cos(\pi j) \quad (10)$$

where A = 1.2798812. According to our calculations the surface layer (j = 0) is the most shortened ($d^{0}_{10.4}$ = 3.0018 Å), whereas the underlying one (j = 1) is the most dilated ($d^{1}_{10.4}$ = 3.1129 Å), when they are compared with the layer placed at the center of the slab ($d^{5}_{10.4}$ = 3.0895 Å).

The trend of $\Delta\mu^{j}_{CaCO3}(298)$ (and $\Delta\mu^{j,0}_{CaCO3}$) is in phase contrast with respect to the one of $\Delta d^{j}_{10.4}$: at the highest $\Delta\mu^{j}_{CaCO3}(298)$ corresponds the lowest $\Delta d^{j}_{10.4}$.

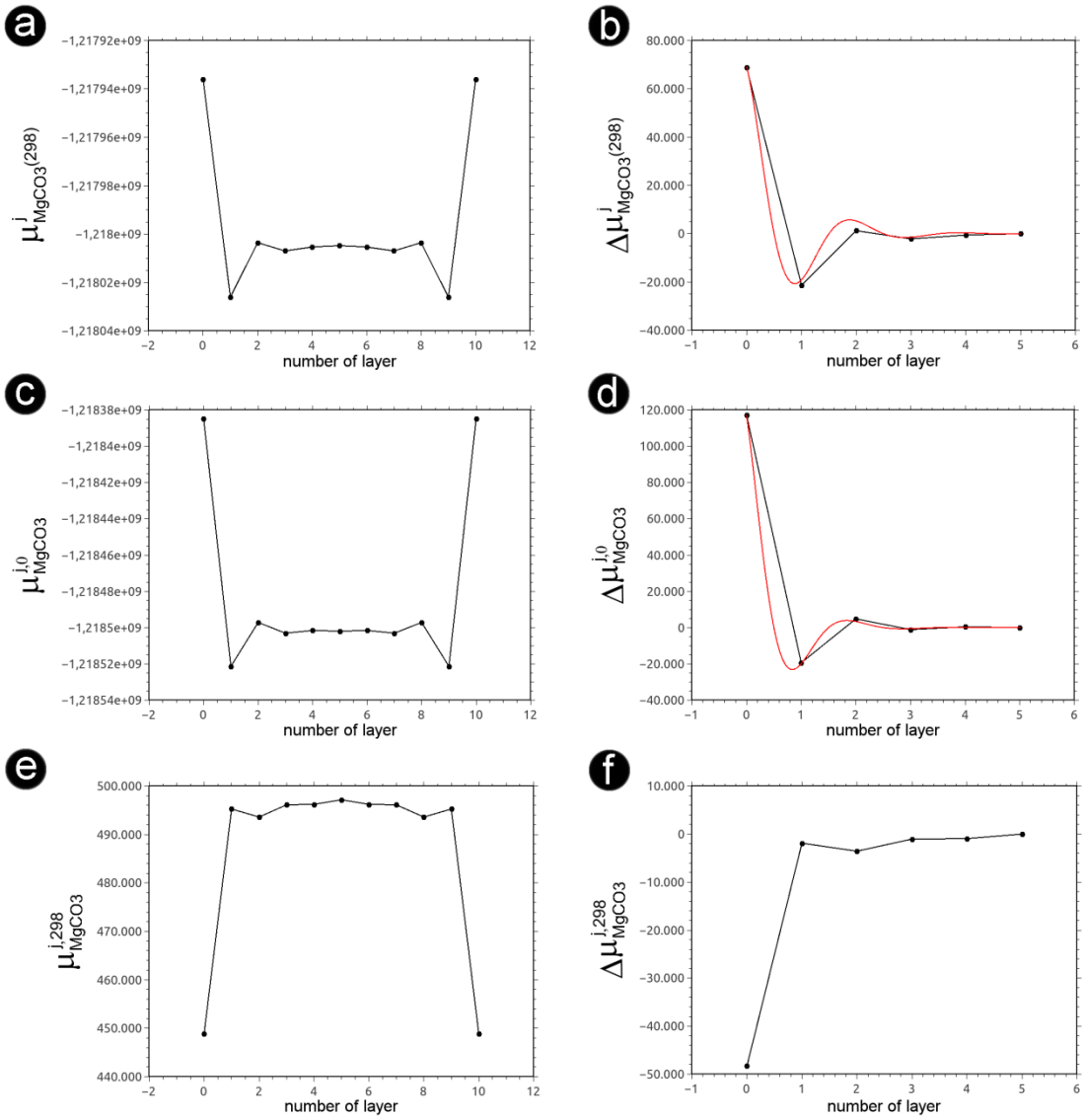

Figure 2. The chemical potential of $MgCO_3$ at 298K (a), $\mu^{j}_{MgCO3}(298)$, its static contribution at 0K (c), $\mu^{j,0}_{MgCO3}$, and its thermal contribution (i.e., vibrational energy and entropy) at 298K (e), $\mu^{j,298}_{MgCO3}$, are reported for each layer j = 0, …, 10 forming the (10.4) slab. The quantities $\Delta\mu^{j}_{MgCO3}(298) = \mu^{j}_{MgCO3}(298) - \mu^{5}_{MgCO3}(298)$ (b), $\Delta\mu^{j,0}_{MgCO3} = \mu^{j,0}_{MgCO3} - \mu^{5,0}_{MgCO3}$ (d) and $\Delta\mu^{j,298}_{MgCO3} = \mu^{j,298}_{MgCO3} - \mu^{5,298}_{MgCO3}$ (f) are also reported. All of the quantities are expressed in J/mol. $\Delta\mu^{j}_{MgCO3}(298)$ and $\Delta\mu^{j,0}_{MgCO3}$ are fitted (red line) with a damped oscillating function, see the main text.

2.5. The chemical potential in the (10.4) slab of magnesite

In Fig. 2 $\mu^{j}_{MgCO3}(298)$, $\mu^{j,0}_{MgCO3}$ and $\mu^{j,298}_{MgCO3}$ are reported; in Table S2 (Supporting Information) the numerical values are listed. As for calcite, the highest value of the chemical potential is associated to the surface layer ($\mu^{0}_{MgCO3}(298)$ = -1.21793602×10^9 J/mol) and the lowest one is in correspondence to layer 1 ($\mu^{1}_{CaCO3}(298)$ = -1.21802608×10^9 J/mol). Also in this case, $\mu^{j}_{CaCO3}(298)$ rapidly converges to the chemical potential of the crystal bulk ($\mu^{5}_{MgCO3}(298) \equiv \mu^{bulk}_{MgCO3}(298)$ = -1.21800480×10^9 J/mol); $\mu^{0}_{MgCO3}(298)$ and $\mu^{1}_{MgCO3}(298)$ that are, respectively, ~0.006% and ~0.002% higher and lower than $\mu^{bulk}_{MgCO3}(298)$. The damped oscillatory behaviour is evident also in the case of magnesite (Tables S2 and S4, Supporting Information): $\Delta\mu^{j}_{MgCO3}(298)$ (Fig. 2b) and $\Delta\mu^{j,0}_{MgCO3}$ (Fig. 2d) are well described by the parameters A = 1.2846754 and A =1.7711952, respectively.

The magnitude and trend of the thermal contribution to the chemical potential of magnesite, $\mu^{j,298}_{MgCO3}$, are quite similar to those of calcite, with the exception of a slight decrease in correspondence of the layer 2 (Figs. 2e and 2f); $\mu^{0,298}_{MgCO3}$ = 4.4884669×10^5 J/mol is lower by 9.4% and 9.7% with respect to $\mu^{1,298}_{MgCO3}$ and $\mu^{5,298}_{MgCO3} \equiv \mu^{bulk,298}_{MgCO3}$, respectively.

Similarly to the calcite case, the DOB of the chemical potential in the (10.4) slab of magnesite is related to the strong variations of the interplanar distances; the quantities $d^{j}_{10.4}$ and $\Delta d^{j}_{10.4} = d^{j}_{10.4} - d^{bulk}_{10.4}$ are plotted in Figs. 3c and 3d, respectively. Their damping behaviour is described by means of eq. (10) and the parameter A = 1.4003017. At the center of the slab the inter-layer spacing is $d^{5}_{10.4}$ = 2.7679 Å, while at the surface the spacing is strongly shortened, $d^{0}_{10.4}$ = 2.6323 Å, and then dilated, $d^{1}_{10.4}$ = 2.8016 Å, at the second layer.

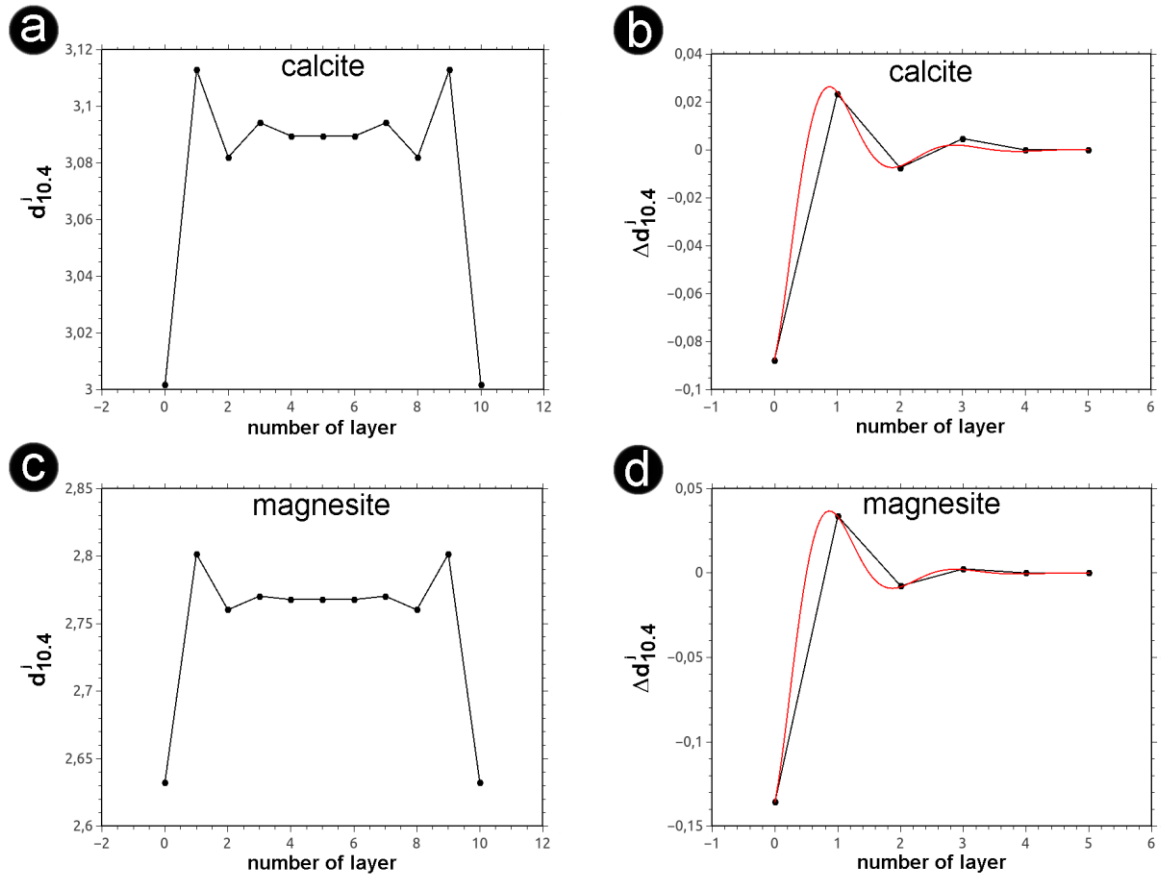

Figure 3. The interplanar distance $d^j_{10.4}$ (Å) for the (10.4) slabs of calcite (a) and magnesite (c) are reported, as well as the quantities $\Delta d^j_{10.4} = d^j_{10.4} - d^5_{10.4}$ (b and d). $\Delta d^j_{10.4}$ is fitted (red line) with a damped oscillating function, see the main text.

3. Conclusions

It is the first time that the behaviour of the chemical potential of a crystal in proximity of its surface is determined at this level of detail. As a consequence, this is also the first time that it is possible to describe the oscillatory behaviour of a fundamental thermodynamic quantity like the chemical potential.

In the following a summary of the results is reported:

(i) The behaviour of $\mu^j_{CaCO3}(298)$ and $\mu^j_{MgCO3}(298)$ inside a (10.4) slab is very similar, even if a slightly more pronounced damping can be observed in the case of calcite, the damping coefficient (A = 1.4302098) being higher than in magnesite (A = 1.2846754). For both the phases the thermal contribution at 298K of the chemical potential is about four order of magnitude lower with respect to the static one.

(ii) The damped oscillatory behaviour (DOB) of the chemical potential is the energy counterpart of the structural modification of the slab caused by the presence of the surface, which produces strong damped oscillatory variations of the interplanar distances. The damped oscillating behaviour of the interplanar distance in proximity of a relaxed surface was already pointed out by others researchers. An interesting paper discussing this phenomenon is that by Houchmandzadeh et al.,[20] where a simplified analytical model is developed to determine the surface relaxation of a crystal. In that work, the DOB behaviour arises for determined values of the model parameters, while a purely exponential decay of the interplanar distance is obtained with different parameters values.

(iii) The features of the free energy density profile of the (10.4) slab of calcite calculated by Bruno[6] by means of the Rohl's force field,[7] were qualitatively well reproduced by our *ab initio* calculations: that is, (i) the highest and lowest values of the chemical potential (and free energy density) are in correspondence of the first and second layer of the slab, respectively; (ii) the chemical potential (and free energy density) of the second layer is lower than that of the crystal bulk.

(iv) The free surface energies at 298K of the (10.4) face of calcite and magnesite result to be γ^{298}_{CaCO3} = 0.459 and γ^{298}_{MgCO3} = 0.452 J/m^2, respectively. The surface energies at 0K are instead γ^{0}_{CaCO3} = 0.508 and γ^{0}_{MgCO3} = 0.501 J/m^2. Then, at 298K the thermal (vibrational) contributions to the free surface energies are equal for the two phases, $\gamma^{298,vib}_{CaCO3} = \gamma^{298,vib}_{MgCO3}$ = -0.049 J/m^2.All these quantities were calculated by eq. (3), as described in detail by Bruno and Prencipe[5] and Bruno.[6] The γ^{298}_{CaCO3} value obtained in this work is in very good agreement with our previous estimate at 300K (γ^{300}_{CaCO3} = 0.464 ± 0.018 J/m^2);[21] in the paper by Bruno et al.,[21] a comparison between experimental and theoretical determinations of the surface energy of the (10.4) face of calcite is also done. Unfortunately, no free surface energy values at 298K of the (10.4) face of magnesite to compare with our result exist. We only found an estimate of γ^{0}_{MgCO3} = 0.256 J/m^2 that was obtained at empirical level by Wright et al.[22]

(v) The equilibrium morphology of a crystal can be composed by several crystallographic forms, whose number and type depend mainly on the temperature and composition of the mother solution. At the equilibrium, the chemical potential of the surface layer must be equal for all of the {hkl} crystallographic forms. The different surface energies associated to the {hkl} forms have a counterpart on the way the chemical potential varies from the surface to the center of the crystal. Then, the surface energies of the crystallographic forms belonging to the

equilibrium morphology can be seen as different damped oscillating functions having yet the same values at their extremes placed at the surface and at the center of the crystal.

(vi) The chemical potential of a chemically homogeneous crystal at the equilibrium at some pressure and temperature, is usually supposed to be constant everywhere inside the phase. But we have demonstrated in this work that this condition cannot be fulfilled for a real crystal, where the surfaces interrupt the 3D periodicity of the phase and perturb the crystal field. In any crystal, both at the equilibrium and far away from the equilibrium, there is always a gradient of the chemical potential in proximity of a surface: the chemical potential homogeneity in a real crystal does not exist.

Acknowledgements

Thanks are due to three anonymous reviewers for their careful reading of the manuscript and their fundamental observations on our work.

Supporting Information Available. Computational details concerning the ab initio simulations of the (10.4) surface of calcite and magnesite; numerical values of the chemical potential of $CaCO_3$ f.u. in the (10.4) slab of calcite at 298K (Table S1); numerical values of the chemical potential of $MgCO_3$ f.u. in the (10.4) slab of magnesite at 298K (Table S2); numerical values of the quantities plotted in Figs. 1b, 1d, 2b and 2d, and fitted (red line) with eq. (9) (Tables S3 and S4). This material is available free of charge via the Internet at http://pubs.acs.org.

References

(1) Holland, T.J.B.; Powell, R. *J. metamorphic Geol.* **2011**, *29*, 333-383.
(2) Hickel, T.; Grabowski, B.; Körmann, F.; Neugebauer, J. *J. Phys.: Condens. Matter* **2012**, *24*, 053202.
(3) Wentzcovitch, R.M.; Yu, Y.G.; Wu, Z. In: Theoretical and Computational Methods in Mineral Physics: Geophysical Applications; Wentzcovitch, R.M.; Stixrude, L., Eds.; Reviews in Mineralogy and Geochemistry, Mineralogical Society of America Geochemical Society, 2010, p. 481.
(4) Gillan, M.J.; Alfè, D.; Brodholt, J.; Vočadlo, L.; Price, G.D. *Rep. Prog. Phys.* **2006**, *69*, 2365-2441.
(5) Bruno, M.; Prencipe, M. *CrystEngComm* **2013**, *15*, 6736-6744.
(6) Bruno, M. *CrystEngComm* **2015**, *17*, 2204-2211.
(7) Rohl, A.L.; Wright, K.; Gale, J.D. *Am. Mineral.* **2003**, ***88***, 921–925.
(8) Dovesi, R.; Civalleri, B.; Orlando, R.; Roetti, C.; Saunders, V.R. In: Reviews in Computational Chemistry; Lipkowitz, B.K.; Larter, R.; Cundari, T.R., Eds.; John Wiley & Sons, Inc.: New York, 2005, vol.1, p.443.
(9) Dovesi, R.; Orlando, R.; Civalleri, B.; Roetti, C.; Saunders, V.R.; Zicovich-Wilson, C.M. *Z. Kristallogr.* **2005**, *220*, 571-573.
(10) Dovesi, R. *et al.*, *CRYSTAL09 User's Manual*; University of Torino: Torino, Italy, 2009.
(11) Pisani, C.; Dovesi, R.; Roetti, C. *Hartree-Fock ab-initio treatment of crystalline systems*, Lecture Notes in Chemistry; Springer: Berlin, Heidelberg, New York, 1988.
(12) Becke, A.D. *J. Chem. Phys.* **1993**, *98*, 5648-5652.
(13) Lee, C.; Yang, W.; Parr, R.G. *Phys. Rev. B* **1988**, *37*, 785-789.
(14) Stephens, P.J.; Devlin, F.J.; Chabalowski, C.F.; Frisch, M.J. *J. Phys. Chem.* **1994**, *98*, 11623-11627.
(15) Bruno, M.; Massaro, F.R.; Prencipe, M.; Aquilano, D. *CrystEngComm* **2010**, *12*, 3626−3633.
(16) Peintinger, M.F.; Oliveira, D.V.; Bredow, T. *J. Comput. Chem.* **2013**, *34*, 451-459.
(17) Weigend, F.; Häser, M.; Patzelt, H.; Ahlrichs, R. *Chem. Phys. Lett.* **1998**, *294*, 143-152.
(18) Weigend, F.; Ahlrichs, R. *Phys. Chem. Chem. Phys.* **2005**, ***7***, 3297-3305.
(19) Valenzano, L.; Noel, Y.; Orlando, R.; Zicovich-Wilson, C.M.; Ferrero, M.; Dovesi, R. *Theor. Chem. Acc.* **2007**, *117*, 991-1000.
(20) Houchmandzadeh, B.; Lajzerowicz, J.; Salje, E. *J. Phys.: Condens. Matter* **1992**, *4*, 9779-9794.
(21) Bruno, M.; Massaro, F.R.; Pastero, L.; Costa, E.; Rubbo, M.; Prencipe, M.; Aquilano, D. *Cryst. Growth Des.* **2013**, *13*, 1170-1179.
(22) Wright, K.; Cygan, R.T.; Slater, B. *Phys. Chem. Chem. Phys.* **2001**, *3*, 839-844.

For Table of Contents Use Only

On the behaviour of the chemical potential in calcite and magnesite crystals: a damped harmonic oscillation

BRUNO Marco,* RUBBO Marco, MASSARO Francesco Roberto

Dipartimento di Scienze della Terra, Università degli Studi di Torino, Via Valperga Caluso 35, I-10125, Italy

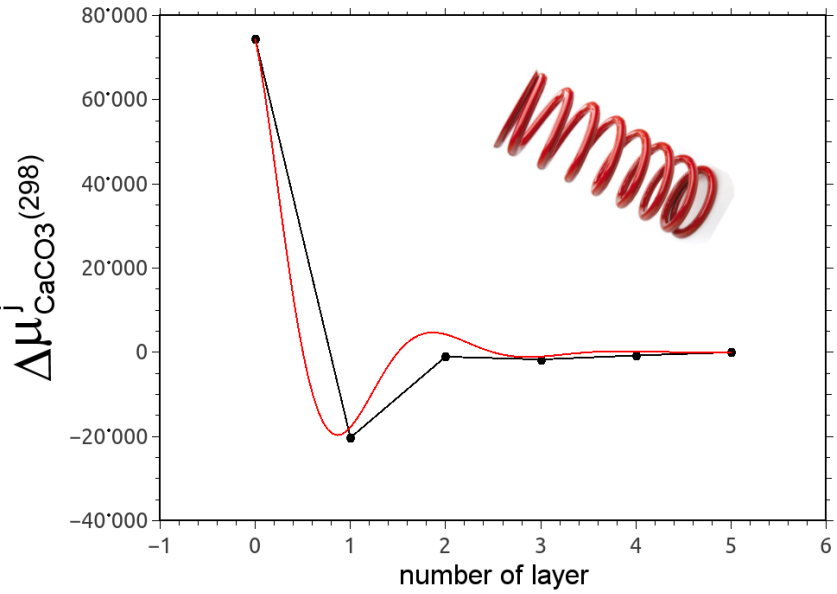

Synopsis

The damped oscillatory behaviour of the chemical potential of the chemical species $CaCO_3$ and $MgCO_3$ in proximity of the (10.4) crystal face of calcite and magnesite, is determined at quantum-mechanical level.